HHS Public Access

Author manuscript

Environ Int. Author manuscript; available in PMC 2023 October 29.

Published in final edited form as:

Environ Int. 2023 October ; 180: 108213. doi:10.1016/j.envint.2023.108213.

Adverse developmental impacts in progeny of zebrafish exposed to the agricultural herbicide atrazine during embryogenesis

Janiel K. Ahkin Chin Tai[a], **Katharine A. Horzmann**[a,b], **Thomas L. Jenkins**[c], **Isabelle N. Akoro**[a], **Sydney Stradtman**[a], **Uma K. Aryal**[d,e], **Jennifer L. Freeman**[a,*]

[a]School of Health Sciences, Purdue University, West Lafayette, IN, USA

[b]Department of Pathobiology, Auburn University, Auburn, AL, USA

[c]Weldon School of Biomedical Engineering, Purdue University, West Lafayette, IN, USA

[d]Department of Comparative Pathobiology, Purdue University, West Lafayette, IN, USA

[e]Bindley Bioscience Center, Discovery Park, Purdue University, West Lafayette, IN, USA

Abstract

Atrazine (ATZ) is an herbicide commonly used on crops in the Midwestern US and other select global regions. The US Environmental Protection Agency ATZ regulatory limit is 3 parts per billion (ppb; μg/L), but this limit is often exceeded. ATZ has a long half-life, is a common contaminant of drinking water sources, and is indicated as an endocrine disrupting chemical in multiple species. The zebrafish was used to test the hypothesis that an embryonic parental ATZ exposure alters protein levels leading to modifications in morphology and behavior in developing progeny. Zebrafish embryos (F1) were collected from adults (F0) exposed to 0, 0.3, 3, or 30 ppb ATZ during embryogenesis. Differential proteomics, morphology, and behavior assays were completed with offspring aged 120 or 144 h with no additional chemical treatment. Proteomic analysis identified differential expression of proteins associated with neurological development and disease; and organ and organismal morphology, development, and injury, specifically the skeletomuscular system. Head length and ratio of head length to total length was significantly increased in the F1 of 0.3 and 30 ppb ATZ groups ($p < 0.05$). Based on molecular pathway alterations, further craniofacial morphology assessment found decreased distance for cartilaginous structures, decreased surface area and distance between saccular otoliths, and a more posteriorly positioned notochord ($p < 0.05$), indicating delayed ossification and skeletal growth. The visual motor response assay showed hyperactivity in progeny of the 30 ppb treatment group for distance moved and of the 0.3 and 30 ppb treatment groups for time spent moving ($p < 0.05$). Due to the changes in saccular otoliths, an acoustic startle assay was completed and showed decreased response in the 0.3 and 30 ppb treatments ($p < 0.05$). These findings suggest that a single

*Corresponding author at: School of Health Sciences, 550 Stadium Mall Drive, West Lafayette, IN 47907, USA. jfreema@purdue.edu (J.L. Freeman).

Declaration of Competing Interest

The authors declare that they have no known competing financial interests or personal relationships that could have appeared to influence the work reported in this paper.

Appendix A. Supplementary material

Supplementary data to this article can be found online at https://doi.org/10.1016/j.envint.2023.108213.

embryonic parental exposure alters cellular pathways in their progeny that lead to perturbations in craniofacial development and behavior.

Keywords

Atrazine; Behavior; Multigeneration; Proteomics; Skeletal; Zebrafish

1. Introduction

Atrazine (ATZ) is a triazine herbicide that is commonly applied to agricultural fields to control broad leafy weeds (LeBaron, McFarland, & Burnside, 2008). Although ATZ is the second most common agricultural herbicide in the US and is used widely in most global regions, the European Union banned its use in 2003 due to water contamination concerns (Bethsass and Colangelo 2006; (European Commission, 2003)). Due to heavy application and low binding efficiency to soils, ATZ contaminates runoff and potable water sources (Guzzella et al. 2006; Meffe and de Bustamante 2014). The US Environmental Protection Agency (EPA) has set the maximum contaminant level of ATZ in potable water to 3 parts per billion (ppb; μg/L), but concentrations can exceed this limit (Blanchard and Lerch, 2000). Moreover, the World Health Organization increased the ATZ regulatory limit in drinking to 100 ppb in 2011 (World Health Orgnanization, 2011).

In the general population, the most common ATZ exposure route is through drinking contaminated water and is associated with several health risks, which have been documented in epidemiological studies as well as various animal studies. Epidemiological studies suggest exposure during gestation increases the likelihood of birth defects and premature births (Agopian et al. 2013; Migeot et al. 2013; Stayner et al. 2017; Waller et al. 2010). For example, women with medium levels of residential ATZ exposure had increased risk of offspring with male genital malformations in Texas, USA (Agopian et al. 2013). In addition, a study in France with women exposed in their second trimester with mixtures of ATZ metabolites and nitrates in their drinking water found their offspring were more likely to be born small for gestational age (Migeot et al. 2013). An assessment of births in counties across the Midwestern US for water systems included in the US EPA's ATZ monitoring program found there was increased rate of preterm birth (Stayner et al. 2017), while a study in Washington, USA found women who resided less than 25 km from a site with high ATZ concentrations had offspring with increased frequency of gastroschisis (Waller et al. 2010). Furthermore, studies in various model organisms support ATZ as an neuroendocrine disrupting compound, altering reproductive cycling and development (Cooper 2000; Weber et al. 2013; Russart and Rhen 2016; Wirbisky et al. 2016b), stress response (Foradori et al. 2018; Fraites et al. 2009; Horzmann et al. 2022), and the dopaminergic system (Bardullas et al. 2011; Fraites et al. 2009; Li et al. 2019; Ma et al. 2015).

Adverse health outcomes with direct ATZ exposure are well documented, but multigenerational and transgenerational studies are important to determine if an exposure affects subsequent generations, and whether the adverse health outcomes are comparable. Moreover, some studies have begun to assess ATZ toxicity in the context of the

Developmental Origins of Health and Disease (DOHaD) paradigm, which states that exposures to environmental factors or chemical exposures during developmental periods can have long lasting impacts into adulthood and even subsequent generations (Heindel and Vandenberg 2015). Transgenerational studies in Sprague Dawley rats at high concentrations support generational effects of ATZ exposure, reporting reductions in body weight, increased testis disease, and early onset puberty in males and in their offspring, as well as hyperactivity and altered methylation patterns in sperm (DeSesso et al. 2014; McBirney et al. 2017). In mice, decreased sperm quality in the generation exposed to ATZ during development and in the following generation due to defects of proteins in meiosis and altered gene expression in several organs was observed (Hao et al. 2016). ATZ exposure during the first 12 days of life in medaka documented decreased sperm count and motility in offspring (Cleary et al. 2019). Previous studies in zebrafish with an embryonic ATZ exposure report alterations in proteins related to development, neurological disorders, and cancer, as well as changes in morphology and genes associated with head development, neurogenesis, and behavior (Horzmann et al. 2018, 2021, 2022; Weber et al. 2013; Wirbisky et al. 2015). Specifically, increased head length was observed at the end of embryogenesis (Weber et al. 2013) with hyperactivity in 0.3 ppb and hypoactivity in 30 ppb treatment groups in the larval visual motor response assay (Horzmann et al. 2018; Ahkin Chin Tai et al. 2021). In addition, the adult zebrafish with embryonic ATZ exposure showed key molecular pathways changed in the brain transcriptome with movement behavior changes in the males and anxiety-related behavior patterns in the females (Horzmann et al., 2021, 2022). Building upon these findings, we expect that an embryonic ATZ exposure in zebrafish will have generational consequences. Specifically, it was hypothesized that offspring of zebrafish exposed to ATZ only during embryogenesis will exhibit similar changes in protein abundance, morphology, and behavior as the parental generation. Zebrafish are an established model in toxicology and environmental health research with several strengths for generational ATZ studies, including high similarity of physiological structures and molecular pathways related to development and disease, ex vivo embryonic development, shorter developmental and generation times, and established behavioral assays (Bailey et al. 2013; Garcia et al. 2016; Horzmann and Freeman 2018; Stradtman and Freeman 2021). In addition, it was confirmed that zebrafish metabolize ATZ similar to mammals producing the same major metabolites (Ahkin Chin Tai et al. 2021).

2. Materials and methods

2.1. Zebrafish husbandry and dosing

Adult zebrafish (Wild-type AB strain *Danio rerio*) were housed in standalone systems (Aquatic Habitats, Apopka, FL) on a 14:10 light—dark cycle and monitored twice daily for water quality. System water was maintained at 28 °C with a pH range of 7.1–7.3 pH and conductivity of 470–550 μS. Adult fish were fed twice daily a combination of brine shrimp, Golden Pearls (500–800 μm) (Artemia International LLC., Fairview, Texas), and Zeigler adult zebrafish food (Zeigler Bros Inc., Gardners, PA). Zebrafish were bred to generate embryos for experiments in breeding tanks according to established protocols (Peterson et al. 2011). Embryos were collected at the 4–8 cell stage of development (1 h post fertilization: hpf), rinsed, and randomly assigned to treatment groups of 0 (aquaria water),

0.3, 3, or 30 ppb (μg/L) ATZ. ATZ stock solutions were prepared from technical grade ATZ (98.1% purity) (CAS 1912-24-9; Chem Service, West Chester, PA) as previously described (Weber et al. 2013; Wirbisky et al. 2015) and diluted to the respective ATZ treatment concentrations. Concentrations of stock solutions and treatment water were confirmed by an US EPA approved immunoassay kit (Abraxis Atrazine ELISA Kit, Warminster, PA) as previously described (Freeman et al. 2005; Wirbisky et al. 2016a) and were found to all be within expected concentration ranges (±0.1 ppb; data not shown).

Embryos were exposed via immersion in groups of 50 in petri dishes at 1 hpf and were housed at 28.5 °C through the end of embryogenesis (72 hpf). At 72 hpf, all eleutheroembryos were rinsed to terminate ATZ treatment and were raised to adulthood under control conditions. The exposure procedure was replicated several times to attain multiple adult groups. The adult zebrafish exposed to ATZ only during embryogenesis (ATZ F0) were then bred within treatment group to generate embryos. These progenies received no additional ATZ exposure and were maintained at 28.5 °C in aquaria water in groups of 50 in petri dishes until 120 hpf or 144 hpf for experimental procedures. All larvae within a single petri dish were considered as a subsample. For all experimental procedures, larvae were collected from multiple petri dishes (biological replicates) from multiple breeding groups. Larvae with parental embryonic ATZ exposure are referred to as ATZ F1. The experimental design with chemical dosing times and analysis time points is summarized in Supplemental Fig. 1. All protocols were approved by the Purdue University Animal Care and Use Committee and all fish treated humanely with regards to prevention and alleviation of suffering.

2.2. Proteomics

Proteomic analysis was performed on larval F1 zebrafish at 120 hpf to determine whether parental exposure resulted in protein abundance alterations using the same experimental parameters as in our previous study (Horzmann et al. 2018). For each biological replicate, 30 larvae per treatment group (parental exposure of 0, 0.3, 3, or 30 ppb ATZ) were pooled and euthanized via hypothermic shock. Six biological replicates were collected for each F1 treatment group. Larval zebrafish were homogenized using a Preceyllys 24 homogenizer (Bertin Instruments, Montignyle-Bretonneux, France) and a Bicinchoninic (BCA) assay used to determine protein concentration. Sample preparation and analysis was completed as described in Horzmann et al. (2018). Briefly, digestions were performed on a Barocycler NEP2320 at 50 °C under 20,000 psi for 1 h and then samples cleaned over C18 spin columns (Nest Group, Southborough, MA) and dried in a vacuum centrifuge. Peptides were solubilized in 97% purified water, 3% acetonitrile (ACN), 0.1% formic acid (FA). Samples were then analyzed through liquid chromatography/mass spectrometry (LC/MS) with the Dionex UltiMate 3000 RSLC Nano System coupled to the Q Exactive™ HF Hybrid Quadrupole-Orbitrap Mass Spectrometer (QE HF; Thermo Scientific, Waltham, MA). Peptides were loaded onto a trap column (20 μm × 350 mm) and washed using a flow rate of 5 μL/min with 98% purified water, 2% ACN, 0.01% FA. The trap column was switched in-line with the analytical column after 5 min, and peptides were separated using a reverse phase Acclaim PepMap RSLC C18 (75 μm × 15 cm) analytical column using a 120 min method at a flow rate of 300 nl/min. Mobile phase A consisted of 0.01% FA in water

while mobile phase B consisted of 0.01% FA in 80% ACN. The linear gradient started at 5% B and reached 30% B in 80 min, 45% B in 91 min, and 100% B in 93 min. The column was held at 100% B for the next 5 min before being brought back to 5% B and held for 20 min. Samples were injected into the QE HF through the Nanospray Flex™ Ion Source fitted with an emission tip (Thermo Scientific). Data acquisition was performed, monitoring the top 20 precursors at 120,000 resolution with an injection time of 100 ms. For quality assurance and quality control, instrument evaluations and calibrations are run weekly and a standard *E. coli* digest (Waters, Milford, MA) is used routinely to check instrument performance.

Data were processed using the MaxQuant computational proteomics platform (Cox and Mann 2008) against *Danio rerio* sequences from UNIPROT and a common contaminants database with MaxQuant default Orbitrap parameters and minimum peptide length of seven amino acids. Data were analyzed with label-free quantification (LFQ) and the 'match between runs' interval set to 1 min. Other analysis settings included protein FDR at 1%, enzyme trypsin and LysC allowing for two missed cleavages and three modifications per peptide. Fixed modifications were iodoethanol and variable modifications were set to acetyl (protein N-term) and oxidation of methionine. An in-house script was used within the MaxQuant results to remove all common contaminant proteins, to log transform [log2(x)] the LFQ intensity values, to input missing values using the average values of the other samples when one sample was missing, and to use half of the lowest intensity when all samples were missing in one group and present in all other samples in the other group.

2.3. Morphology measurements

F1 ATZ larvae from each parental treatment group were assessed to determine if morphology was altered at 120 hpf. Larvae were euthanized via anesthetic overdose with 0.4 mg/ml buffered tricaine-S (Western Chemical Inc.). For each F1 treatment group, 10–13 larvae were imaged as subsamples per biological replicate. A total of 8 biological replicates were assessed to total 80–100 larvae per treatment group. Measurements assessed were total body length, head length, head width, and brain length similar to our previous study (Horzmann et al. 2018). Total body length was measured dorsally from the top of the head to the caudal fin. Head width was measured dorsally as the distance between the widest part of the eyes. Head length was measured dorsally from the top of the head to the beginning of the yolk sac protrusion. Brain length was measured as the distance rostrally to the brainstem spinal cord junction (Peterson et al. 2013). Additionally, ratios of head length to body length, head width to body length, and brain length to body length were also assessed for relative comparison. Treatment groups were randomized and blinded during measurement. Images were collected via light microscopy using a Nikon SMZ1500 dissecting microscope with a Nikon Digital Sight DS-fil camera and NIS Elements imaging software (Nikon Instruments Inc., Melville, NY).

2.4. Craniofacial morphology staining and measurements

To determine if craniofacial skeletal or cartilage morphology was altered, alcian blue and alizarin red costaining was completed. At 120 hpf, larvae were euthanized via anesthetic overdose as described above, and then stained simultaneously for alcian blue and alizarin red based on a previously established protocol (Walker and Kimmel 2007). Briefly, samples

were fixed in paraformaldehyde, washed to cease fixation in a series of washes, stained with alcian blue overnight, bleached, and stained for alizarin red. After staining, fish were imaged on an Olympus SZX16 dissecting microscope. Images were taken using Cellsentry (Waltham, MA) and structures measured using ImageJ. Cartilaginous structures were assessed based on previously described protocols (Cohen et al. 2014; Staal et al. 2018; Walker et al. 2018) and included palatoquadrate cartilage (PQ) length, Meckel's length, ceratohyal cartilage (CH) angle, Meckel's angle, the distance between the CH and Meckel's structure, the angle between PQ and CH, the angle between PQ and Meckel's angle, and jaw distance (Supplemental Fig. 2). For skeletal structures, surface area of the utricular and saccular otoliths, length between the utricular otoliths and between the saccular otoliths, parasphenoid, notochord, and notochord to jaw length were measured as in previous studies (Aceto et al. 2015; Luo et al. 2016) (Supplemental Fig. 3). For each F1 treatment group 11–20 larvae were imaged as subsamples per biological replicate. A total of 5 biological replicates were assessed to achieve 55–75 larvae per treatment group.

2.5. Larval visual motor response assay

A larval visual motor response test was performed at 120 hpf to determine if F1 larvae exhibited altered behavior from parental ATZ exposure following an established protocol (Horzmann et al. 2018, Ahkin Chin Tai et al. 2021). Each larvae was individually placed into a 96 square well plate in 0.5 mL of aquaria water. Larvae were acclimated for 10 min at 28 °C in the Noldus DanioVision Observation Chamber (Noldus Information Technology, Wagenningen, Netherlands). The Noldus white light routine consisting of alternating 10 min of dark and white light to test the visual motor response was performed over 50 min (3 dark phases and two light phases). Behavioral experiments were performed between 11 am to 1 pm to minimize circadian variability in movement. Infrared movement was recorded during behavioral experiments at a rate of 25 frames per second with a Basler GenICam acA 1300–60 g camera and analyzed with Noldus EthoVision 12.0 software. Tracks were smoothed for total distance moved, velocity, and time spent moving. Each treatment group (0, 0.3, 3, or 30 ppb ATZ F1) had 8 biological replicates containing 24 subsample fish per biological replicate for a total of 192 fish per treatment group.

2.6. Larval acoustic startle response assay

An acoustic startle response assay (ASR) was performed at 144 hpf to determine if parental ATZ exposure caused alterations to vibrational/sound stimuli, as well as habituation. Similar to the visual motor response assay, larvae were placed individually into a 96 square well plate in 0.5 mL of aquaria water and acclimated for 10 min in the Noldus DanioVision Observation Chamber at 28 °C prior to beginning the test (Noldus Information Technology, Wagenningen, Netherlands). The ASR assay consisted of 10 min of recording time in the dark light settings (Fitzgerald et al. 2019) with an acoustic stimulus every 2 min. The acoustic stimulus was run through the Daniovision acoustic startle response stimulus at level 8, with an inter-stimulus interval of 2 min for a total of 10 min similar to as previously described (Pantoja et al. 2016). Behavioral experiments were performed between 11 am to 1 pm to minimize circadian variability in movement. Infrared movement was recorded at 60 frames per second with a Basler GenICam acA 1300–60 g camera. Behavioral data was analyzed on Noldus EthoVision 12.0 software with smoothed tracks for total distance,

velocity, and time spent moving. A total of 5 replicates consisting of 24 subsamples per treatment group in each biological replicate was included to total 120 total larvae per treatment group. Once experiments were completed, a Matlab code was made to quantify C-bends.

2.7. Statistics

For each experiment, one spawning event represents one biological replicate with fish within a single petri dish considered as subsamples. Multiple spawning events from multiple groups of ATZ exposed adults were included among the biological replicates for all experimental procedures. For proteomics, statistical analysis was performed in R. A one-way analysis of variance (ANOVA) was performed on the LFQ intensities and proteins with a p-value < 0.05 were analyzed with a Tukey's post hoc test to identify differences between treatment groups. The list of significantly altered proteins was imported into Ingenuity Pathway Analysis (IPA; Qiagen, Germantown, MD) and matched to the human orthologs of the zebrafish proteins for gene ontology and molecular pathway analysis.

For morphology and behavior, statistics were performed in SAS Statistical Software (SAS Institute Inc. Cary, NC). A Grubb's outlier test was used to detect outliers within treatment groups for morphology and behavior. All data was assessed and confirmed for normality before further statistical analysis. An ANOVA was used to analyze differences in morphological measurements and ASR locomotor behavior among treatment groups and a Fisher's least significant difference (LSD) test at $\alpha = 0.05$ was incorporated when a significant ANOVA was observed. For phasic behavioral analysis of the visual motor response assay a repeated measures ANOVA was used to assess phase, treatment, and the interaction of phase*treatment. Similarly, a repeated measures ANOVA was also used to analyze C-bends by tap. All behavioral data is represented in bar graphs (Bridi et al. 2017; Horzmann et al. 2018). All results are presented as mean ± standard deviation of the mean.

3. Results

3.1. Proteomic alterations in progeny

A total of 1,277 unique proteins were identified (Supplemental Table 1). From this list, 62 proteins had significant LFQ intensity values ($p < 0.05$) in larvae of the F1 0.3 ppb treatment group, while 32 and 24 proteins were significantly altered in larvae of the 3 and 30 ppb treatment groups, respectively. In IPA, 54 of the 62 proteins in the F1 0.3 ppb treatment group, 26 of the 32 proteins in the 3 ppb treatment group, and 20 of the 24 proteins in the 30 ppb treatment group were recognized for mapping to their human ortholog (Fig. 1). These 100 significant calls consisted of 70 unique mapped proteins including several ATP synthase proteins (ATP5F1A, ATP5F1C, ATP5MD, ATP5ME, ATP5MG, and ATP5PB), collagen proteins (COL10A1, COL18A1, and COL1A1), heterogeneous nuclear ribonucleoproteins (HNRNPM, HNRNPR, and HNRNPU), and ribosomal proteins (RPL10A, RPL11, RPL17-C18orf32, RPL3, RPL4, RPS11, RPS16, and Rps3a1) (Table 1). 24 proteins were altered in two treatment groups (23 proteins in the 0.3 and 3 ppb and 1 protein in the 0.3 and 30 ppb treatment groups) and 3 proteins were altered in all three treatment groups (HBE1, MATN3, and SF3B3) (Fig. 1).

Pathway analysis was completed on the mapped proteins within each treatment group to determine molecular pathways altered in the progeny. As expected with a high degree of similarity in proteins altered in the progeny of the 0.3 and 3 ppb treatment groups, similar pathways were altered among these two groups. The top physiological system development and function pathways in the 0.3 and 3 ppb treatment group offspring included embryonic and organismal development, organ development and morphology, and nervous system development and function (Table 2). There were more differences in the top disease and disorder pathways that were altered in the F1 0.3 and 3 ppb treatment groups, although neurological disease and organismal injury and abnormalities were similar (Table 3). In addition, psychological disorders, skeletal and muscular disorders, ophthalmic disease, and cancer were also top pathways. Progeny of the 30 ppb treatment group had some similarities with the other two treatment groups (e.g., organismal injury and abnormalities and cancer), but also hit on reproductive system development and disease. Progeny from the F1 30 ppb had some similarity to the other F1 groups, but there was limited analysis due to a small number of molecular targets within the F1 30 ppb pathways. The F1 30 ppb larvae had a limited number of pathway targets identified, so pathway analysis was not able to be completed.

Upstream regulator and causal pathway analysis identified similarities in the 0.3 and 3 ppb treatment group offspring in DDX5 (DEAD-box helicase 5; 0.3 ppb: p-value: 7.92E-06; 3 ppb: p-value: 8.25E-09) and MYCN (MYCN proto-oncogene; 0.3 ppb: p-value: 2.39E-05; 3 ppb: p-value: 2.70E-04). Top canonical pathways in the 0.3 and 3 ppb treatment group progeny included estrogen receptor signaling, oxidative phosphorylation, and mitochondrial dysfunction.

3.2. Morphological changes in progeny

Length measurements were assessed at 120 hpf (Table 4). A significant increase in mean head length was seen in offspring of the 0.3 and 30 ppb treatment groups ($p < 0.05$). No other changes were seen in total length, mean brain length, or mean head width in the larvae ($p > 0.05$). For morphological ratios to assess relative size compared to total body length, a significant increase was observed in head length to total body length ratio in the offspring of the 0.3 ppb and 30 ppb treatment groups ($p < 0.05$), indicating head length was greater than would be expected based on body length. No significant differences in brain length to total body length or head width to total body length was observed ($p > 0.05$).

3.3. Cartilage and skeletal modifications in progeny

Cartilaginous and skeletal structures were measured at 120 hpf. For cartilaginous structures (Supplemental Fig. 2), PQ length was decreased in all parentally exposed groups ($p < 0.05$, Fig. 2A). In addition, the CH-Meckel's length ($p < 0.05$; Fig. 2B) and jaw distance was decreased in the progeny of the 30 ppb treatment group ($p < 0.05$; Fig. 2C). No differences were detected in the Meckel's angle, PQ-Meckel's angle, CH angle, PQ-CH angle, or Meckel's length ($p > 0.05$) (Supplemental Fig. 4). For skeletal structures (Supplemental Fig. 3), decreased surface area of the saccular otoliths was seen in the progeny of the 30 ppb treatment group ($p < 0.05$; Fig. 3A–B), but no differences observed in utricular otolith areas in the progeny ($p > 0.05$; Fig. 3C–D). Distance between the saccular and utricular otoliths

was also measured. The F1 larvae of the 30 ppb treatment group had decreased distance between the two saccular otoliths ($p < 0.05$; Fig. 3E), but no changes in distance for utricular otoliths ($p > 0.05$; Fig. 3F) was observed. In addition, larvae of the 30 ppb treatment group had a significant posteriorly positioned notochord as measured from the jaw (i.e., notochord to jaw length) ($p = 0.0149$; Fig. 4A), but no difference in the area of the notochord or parasphenoid was observed ($p > 0.05$; Fig. 4B–C).

3.4. Visual motor response in progeny

Phasic behavioral data was assessed for each light and dark period. For phasic total distance, there was significance for phase ($F(5,2450) = 1805.42$, $p < 0.05$), treatment ($F(3,490) = 7.18$, $p < 0.05$), and phase*treatment ($F(15,2450) = 2.09$, $p < 0.05$; Fig. 5A). The 30 ppb F1 progeny moved more total distance in all light and dark phases. For time spent moving, phase ($F(5,2450) = 2408$, $p < 0.05$), treatment ($F(3,490) = 8.64$, $p < 0.05$), and phase*treatment ($F(15,2450) = 3.59$, $p < 0.05$) were significant. Both the 0.3 ppb and 30 ppb F1 progeny spent more time moving in all light and dark phases (Fig. 5B). No significant differences were observed in velocity for treatment ($F(3, 490) = 1.55$, $p > 0.05$) or phase*treatment ($F(15, 2450) = 0.79$, $p > 0.05$; Fig. 5C).

3.5. Acoustic startle response in progeny

Acoustic startle behavioral data was assessed for total distance moved, time spent moving, velocity, and counterclockwise and clockwise movement (Fig. 6). For total distance moved ($p < 0.05$), velocity ($p < 0.05$), and time spent moving ($p < 0.05$), 0.3 and 30 ppb ATZ F1 larvae spent significantly less time moving than controls. The ATZ F1 fish in the 0.3 and 30 ppb treatment groups also spent less time making counterclockwise and clockwise turns in comparison to controls ($p < 0.05$). C-bends were assessed using Matlab software program to determine whether larvae were habituating to a series of tap responses throughout the experiment and was found to be significant ($p < 0.05$; Table 5). No significant changes were found in taps 1, 2, or 3 ($p > 0.05$), but tap 4 had a decrease in C-bend response for 30 ppb ATZ F1 larvae ($p < 0.05$).

4. Discussion

ATZ is an endocrine disrupting chemical that targets the neuroendocrine system resulting in developmental and reproductive consequences as reported in several epidemiological (Agopian et al. 2013; Migeot et al. 2013; Stayner et al. 2017; Waller et al. 2010) and animal model studies (DeSesso et al. 2014; Foradori et al. 2018; Hao et al. 2016; McBirney et al. 2017; Russart and Rhen 2016; Stradtman and Freeman 2021). Multi- and transgenerational studies have shown changes in sperm quality, hyperactivity, and change in weight in subsequent generations, warranting further studies into generational adverse health impacts (Cleary et al. 2019; McBirney et al. 2017). Here, we first used a proteomics approach to identify altered protein levels and molecular pathways in the ATZ F1 larvae. A total of 1,277 unique proteins were identified, which is similar to the total number of proteins detected in past studies (Horzmann et al. 2018), but does only represent a percent of the total proteins in the zebrafish. Regardless, imperative details on altered protein abundance and molecular pathways were ascertained in this study. Overall, more differentially abundant

proteins were observed in progeny of the lowest ATZ treatment group (0.3 ppb). In addition, all proteins altered in offspring of the 3 ppb treatment group were also observed in the 0.3 ppb treatment group. Three proteins were common among all treatment groups: HBE1, MATN3, and SF3B3. HBE1 is an embryonic hemoglobin protein, which suggests changes in oxygen regulation with ATZ exposure (Aceto et al. 2015). MATN3 is an extracellular matrix protein expressed in the cartilage during development (Pullig et al. 2002). Pathogenic variants or alterations in MATN3 abundance are associated with bone disorders in humans, such as multiple epiphyseal dysplasia (MED), which affects the epiphsyses in long bones (Jackson et al. 2012; Pettersson et al. 2018), or osteoarthritis later on in life. SF3B3 is a component of U2 small nuclear ribonucleoprotein-associated protein complex SF3B (Das et al., 1999). SF3B3 is present in the nucleus and partakes in DNA and RNA maintenance and function, including chromatin modification, transcription, splicing, and DNA repair (Chen et al. 2017; Metselaar et al. 2021). Alterations in SF3B3 are linked with carcinogenesis (Chen et al. 2017). Furthermore, SF3B3 was identified along with HNRNPM (altered in offspring of the 30 ppb treatment group in the current study) to interact with RANBP9 (RAN--binding protein 9) in the testis to regulate alternative splicing in spermatogenic cells (Bao et al. 2014). This function is critical for normal spermatogenesis and male fertility, aligning with past studies on ATZ endocrine disrupting properties (Hao et al. 2016; McBirney et al. 2017; Cleary et al. 2019).

Several differentially abundant proteins in the ATZ F1 were within similar families including the ATP synthase proteins, collagen proteins, heterogeneous nuclear ribonucleoproteins, and ribosomal proteins. Past studies identified ATZ to alter ATP content, mitochondrial dysfunction, and collagen fibers and structures in multiple tissues in the initial exposed generation (Lim et al., 2009). The results of the current study indicate these targets are also altered in the subsequent generation. The heterogeneous nuclear ribonucleoproteins are complexes of RNA and protein that serve as a signal that the pre-mRNA is not yet processed; thus, being important for pre-mRNA processing and other aspects of mRNA metabolism and transport. The heterogeneous nuclear ribonucleoproteins localize to border regions of chromatin and are reported to function in multiple cellular processes (Fakan et al. 1984). Moreover, a number of ribosomal proteins were also altered in the ATZ F1 larvae. Ribosomal proteins are highly conserved regulators of translation. Ribosomal proteins altered in the ATZ F1 included both large and small subunits with a number of them known to be associated with Diamond-Blackfan Anemia and/or Shwachman-Diamond Syndrome (RPL11, RPL3, RPL4, RPS11). Although these disorders are inherited conditions, it may suggest similar adverse health targets (e.g., effects on growth, bone marrow, the skeletomuscular system, and/or osteosarcoma) for further study. Pathway analysis of the altered proteins identified associations with neurological development and disease and cancer as well as molecular pathways associated with organ and organismal morphology, development, and injury. These pathways align with many of the adverse health outcomes and molecular pathways indicated to play a role in atrazine toxicity in the exposed generation (F0), including our past proteomic study in the ATZ F0 larvae (Horzmann et al. 2018). These common molecular pathways altered in the exposed (F0) and subsequent (F1) generation included nervous system development, cancer, and organismal injury and abnormalities.

When comparing the specific proteins altered in the ATZ F1 larvae to the ATZ F0 larvae in our previous study, a higher number of proteins were differentially abundant in the larval progeny compared to the same aged larvae that had the embryonic ATZ exposure (ATZ F0) (Horzmann et al. 2018). There was only one common protein altered, ADD3 (adducin 3), in both generations. ADD3 is one of the family members of the adducins. The adducins are associated with membrane skeletal proteins and are involved in the spectrin-actin network in erythrocytes and in epithelial tissues at sites of cell-to-cell contact. In addition, members of the profilin family were also changed in both generations (F0: PFN2L; F1: PFN1). Profilins are also associated with the actin cytoskeleton and are essential for organ development. Mutations in PFN1 are linked to amyotrophic lateral sclerosis (ALS), while overexpression is associated with cancer (Alkam et al. 2017). One previous protein study in MCF-10A human breast epithelial cells also identified PFN1 to be differentially expressed with ATZ exposure (Huang et al. 2014).

Upstream regulator and causal pathway analysis of the differentially abundant proteins identified similarities in the 0.3 and 3 ppb treatment group offspring in the regulator DDX5. DDX5, a putative RNA helicase, is part of the estrogen receptor signaling canonical pathway (also one of the top canonical pathways enriched in these treatment group offspring) involved in embryogenesis, spermatogenesis, and cellular growth and division (Legrand et al. 2019). Overall, this finding along with the other discussed proteome results greatly overlap with the wealth of literature on ATZ's association with the estrogen pathways and endocrine disrupting properties.

Morphology measurements were completed to assess impacts to larval growth parameters and brain development. An increase in head length, along with an increase in head length to total body length ratio were observed, indicating head size was larger than would be expected based on total larval length. These findings agree with an earlier study reporting an increased head length when measurements were completed at 72 hpf immediately following embryonic ATZ exposure in zebrafish (F0) (Weber et al. 2013). Epidemiological studies have also reported alterations in head size and other birth defects related to in utero ATZ exposure (Chevrier et al. 2011; Stayner et al. 2017; Winchester et al. 2009). In addition, zebrafish studies using the DOHaD paradigm, report that an embryonic ATZ exposure leads to altered body weight at 14 months of age in adult female and male zebrafish exposed to ATZ during embryogenesis ((Horzmann et al., 2021, 2022) and altered brain to body weight ratio in adult female zebrafish aged 8 months with exposure to 0.3 or 30 ppb ATZ during embryogenesis (Wirbisky et al. 2016b). Progeny from these same treatment groups (0.3 and 30 ppb ATZ) showed morphological alterations in the current study. Alternatively, when the F0 were exposed to ATZ from 1 to 120 hpf no significant differences in morphology were observed (Ahkin Chin Tai et al. 2021). This discrepancy may be due to the difference in exposure periods between the earlier discussed studies and the current study (i.e., 1–72 hpf) with those exposed from 1 to 120 hpf. Future work is needed to address this question, along with the impacts of these morphological changes as the organisms age.

Based on the molecular pathways identified in the proteomic analysis, further morphological analysis of craniofacial structures was completed. Cranioskeletal formation is conserved among vertebrates (Kuratani et al.) and bone remodeling and signaling in zebrafish and

humans are also similar (Kwon et al. 2019; Mork and Crump 2015; Paul et al. 2016). Zebrafish are an established model for bone remodeling and bone disease modeling (Carnovali et al. 2019; Kwon et al. 2019), making them an ideal organism to understand how ATZ alters craniofacial structures. Furthermore, endocrine disrupting chemicals can cause changes in cartilage and bone development. A couple studies in different model organisms support developmental ATZ exposure interfering with craniofacial bone and cartilage formation during development, including reports in frogs (Lenkowski and McLaughlin 2010) and zebrafish (Walker et al. 2018). In addition, a study with developmental ATZ exposure in chick embryos also showed neural tube defects and craniofacial hypoplasia (Joshi et al. 2013). Conversely, a developmental exposure in South American river turtles found no visual changes with ATZ exposure in whole body skeletal structures (dos Santos Mendonça et al. 2016).

In zebrafish, chondrogenesis is present 2 days after fertilization (48 hpf) and cartilaginous structures begin to develop around 3 days post fertilization (72 hpf) (Kimmel et al. 1998). Cranial bone development in the zebrafish starts from 3 days after fertilization (72 hpf) (Cubbage and Mabee 1996). The jaw is derived from 7 pharyngeal arches by 5 days post fertilization (120 hpf) in the larval zebrafish and neural crest cells during development play a critical role in neurocranial cartilage and bone development. Malformations in the jaw are associated with bone formation or neural crest migrations issues (Kimmel et al. 1998; TeSlaa et al. 2013; Ton et al. 2006). Here, we observed a significant decrease in PQ length for progeny of all ATZ treatment groups and in CH-Meckel's length, jaw distance, and a more posteriorly positioned jaw as measured from the notochord in offspring of the 30 ppb ATZ treatment group.

In addition, a decrease in surface area of the saccular otoliths and a decrease in distance between the saccular otoliths was measured in the offspring of the 30 ppb treatment group, suggesting a decrease in ossification. During the first week of development, zebrafish have only two pairs of otoliths; the utricle, which is anteriorly positioned, and the saccule, which is more posterior. Otoliths are important for hearing and balance in zebrafish. Although these two sets of otoliths are similar in appearance and structure, the utricular otoliths are the crucial vestibular organs (Riley and Moorman 2000) and the saccular otoliths play a major role in hearing, especially in the first week of development (Yao et al. 2016). Zebrafish at 120 hpf are capable of detecting sound and regulating balance (Best et al. 2008; Inoue et al. 2013). Weberian ossicles are present at later developmental stages in zebrafish and are important for detection of sound pressure (Grande and Young 2004). During the first week of development for zebrafish, since Weberian ossicles are not present, the fish compensate with a larger saccular otolith for sound pressure detection and the growth of this otolith is highly regulated during development (Inoue et al. 2013). The smaller surface area of the saccular otoliths as well as decreased distance between the saccular otoliths measured in the current study, again suggest a decrease in ossification with a potential impact to hearing.

These morphological observations are comparable to the craniofacial hypoplasia reported in developing chicks exposed to N-nitrosoatrazine (Joshi et al. 2013). In addition, the current study agrees with two other zebrafish studies reporting decreased ossification of vertebrae in developmentally exposed zebrafish at 8 days post fertilization (Walker et al. 2018) and a

visible phenotype of an underdeveloped jaw at 96 hpf (Ton et al. 2006). Alternatively, the decrease in size of various cartilaginous structures in the 30 ppb ATZ F1 treatment group at 120 hpf contradicts another study in zebrafish in which the authors found a trend of increasing size of cartilaginous structures at 120 hpf (Walker et al. 2018). However, this study was completed in the exposed generation (F0), in which zebrafish were exposed from 8 to 120 hpf to ATZ in a mixture. Overall, the findings in the current study suggest that ATZ exposure in the parental generation can alter craniofacial development in their progeny with alterations observed in cartilaginous and skeletal structures, along with supporting molecular pathway alterations identified in the proteomic analysis.

ATZ as an endocrine disruptor has also been shown to cause sex specific behavioral outcomes in various model organisms. A study in tadpoles observed hyperactivity in ATZ exposed tadpoles, and these tadpoles were also less likely to avoid predatory chemical cues (Ehrsam et al. 2016). A gestational ATZ exposure in C57BL/6 mice found dams had decreased novel object recognition and displayed hyperactivity, while juvenile offspring were hyperactive with an increase in anxiety-like behavior (Lin et al. 2014). Furthermore, a transgenerational ATZ study in Sprague Dawley rats found the F3 generation displayed hyperactivity (McBirney et al. 2017), showing behavioral changes can be observed in subsequent generations. In zebrafish, embryonic ATZ exposure resulted in altered transcriptome pathways associated with behavioral, cognitive, and locomotive changes at 72 hpf (Wirbisky et al. 2016b). Proteomic analysis at 120 hpf in zebrafish exposed to ATZ during embryogenesis (1–72 hpf) also supported molecular pathway alterations associated with behavior, similar to the current study (Horzmann et al. 2018). Furthermore, behavioral analysis with the visual motor response assay in the ATZ F0 zebrafish exposed during embryogenesis (1–72 hpf) showed cumulative hypoactivity in the 30 ppb treatment group at 120 hpf (Horzmann et al. 2018). When the ATZ exposure was extended through 120 hpf in the F0 and locomotion was evaluated by phase, hypoactivity was observed in the 30 ppb treatment group in the dark phases for total distance moved and hyperactivity observed in the 0.3 ppb treatment group in the first light phase in total distance moved and time spent moving (Ahkin Chin Tai et al. 2021). No significant changes were seen for velocity. These findings are similar to what was observed in the current study in the visual motor response assay in the ATZ F1 larvae at 120 hpf, with behavioral alterations only observed in progeny of the 0.3 and 30 ppb treatment groups and no significant changes in velocity, although hyperactivity was observed in the 30 ppb treatment group progeny.

Furthermore, based on the alterations observed in the saccular otoliths, an acoustic stimulus response (ASR) assay was included to investigate potential impacts to sound and vibration in the F1 larvae. The ASR assay was performed at 144 hpf since zebrafish are capable of detecting sound and regulating balance after 120 hpf. In addition, past research indicates this developmental age to be optimal for this assessment (Best et al. 2008; Inoue et al. 2013; Pantoja et al. 2016). A decreased startle response was observed primarily in the 0.3 and 30 ppb ATZ F1 progeny for all endpoints in this study, aligning with the same treatment groups with altered behavior in the visual motor response assay in this study in the F1 and in past studies in the F0 (Ahkin Chin Tai et al. 2021; Horzmann et al. 2018). ASR can activate calcium signals in the serotonergic dorsa raphe nuclei (Pantoja et al. 2016), suggesting that dysregulation of ASR affects the serotonergic system. A previous study

in our laboratory showed adult female F0 zebrafish had decreased serotonin turnover and serotonergic metabolite 5-HIAA (Wirbisky et al. 2015) and adult male F0 zebrafish had decreased numbers of cells in raphe populations (Horzmann et al 2021) when exposed to ATZ only during embryogenesis.

ASR is conserved in vertebrates and the assay also permits identification of changes in habituation levels, which are associated with behavioral and anxiety disorders in humans being critical for adaptive behavior and learning (Pantoja et al. 2016). In zebrafish, a reduction to startle response with a series of tap startles was demonstrated previously in larvae (Best et al. 2008). In this study, C-bends were measured to determine whether larvae were habituating to a series of tap responses throughout the experiment. Decreased C-bends as the tap experiment progressed in progeny of the ATZ 30 ppb treatment group was detected, suggesting altered non-associative learning behavior. Intra-individual and population level variation for C-bends is known to occur (Fitzgerald et al. 2019; Pantoja et al. 2016), meaning that an individual that responds to tap 1 may not respond to tap 2, and so forth, and the power of our study captures the biological variation of this behavior. Furthermore, the ability to habituate to short term startle responses has been shown to have a heritable component since offspring of animals with a high habituation index also were observed to have a high habituation index and vice versa in a past zebrafish study (Pantoja et al. 2016). These observations agree with studies showing that ATZ exposure alters learning and anxiety-related behavior in adult rats (Bardullas et al. 2011), developmentally exposed rats (Wang et al. 2019), and adult zebrafish exposed to ATZ during embryogenesis (Horzmann et al 2022). Moreover, in the context of previous laboratory studies, as well as various developmental transgenerational studies of ATZ exposure, the current study falls in line with the DOHaD exposure model. This paradigm indicates that exposures during development can have long lasting impacts seen later on in life and potentially even in subsequent generations. As such integrating findings of the current study with past observations, heritability of molecular changes leading to serotonergic dysregulation and alterations in cartilage and skeletal structures resulting in the observed impacts on behavioral outcomes is supported for the progeny of the zebrafish exposed to ATZ only during embryogenesis. In addition, the current study agrees with past studies in humans, rodents, and other organisms that developmental ATZ exposures at or around the current regulatory concentration in US drinking water (3 ppb) and well below that of the WHO (100 ppb) is suffice to alter morphological growth parameters and behavior, warranting continued assessment to better understand the health risks of these observations.

Supplementary Material

Refer to Web version on PubMed Central for supplementary material.

Acknowledgements

The authors acknowledge the use of the Purdue Proteomics Facility, Bindley Bioscience Center, a core facility of the NIH-funded Indiana Clinical and Translational Sciences Institute. We especially thank Victoria E. Hedrick and Tiago J.P. Sobreira for their assistance.

Funding

This work was supported by the National Institutes of Health, National Institute of Environmental Health Sciences (R03 ES030545 and R21 ES034966) (JLF), the Indiana Clinical and Translational Sciences Institute (funded in part by Award Number UL1TR002529 from the National Institutes of Health, National Center for Advancing Translational Sciences, Clinical and Translational Sciences Award) (JLF), a Purdue Office of Undergraduate Research (IA), and as part of AgSEED Crossroads funding to support Indiana's Agriculture and Rural Development (JLF).

Data availability

Data will be made available on request.

References

Aceto J, Nourizadeh-Lillabadi R, Marée R, Dardenne N, Jeanray N, Wehenkel L, et al. , 2015. Zebrafish Bone and General Physiology Are Differently Affected by Hormones or Changes in Gravity. Witten PE, ed PLoS ONE 10, e0126928; doi: 10.1371/journal.pone.0126928. [PubMed: 26061167]

Agopian AJ, Lupo PJ, Canfield MA, Langlois PH, 2013. Case-Control Study of Maternal Residential Atrazine Exposure and Male Genital Malformations. Am. J. Med. Genet. 161, 977–982. 10.1002/ajmg.a.35815.

Ahkin Chin Tai JK, Horzmann KA, Franco J, Jannasch AS, Cooper BR, Freeman JL, 2021. Developmental atrazine exposure in zebrafish produces the same major metabolites as mammals along with altered behavioral outcomes. Neurotoxicol. Teratol. 85, 106971. 10.1016/j.ntt.2021.106971. [PubMed: 33713789]

Alkam D, Feldman EZ, Singh A, Kiaei M, 2017. Profilin1 biology and its mutation, actin(g) in disease. Cell. Mol. Life Sci. 74, 967–981. 10.1007/s00018-016-2372-1. [PubMed: 27669692]

Bailey J, Oliveri A, Levin ED, 2013. Zebrafish model systems for developmental neurobehavioral toxicology: Zebrafish Developmental Neurobehavioral Toxicology. Birth Defect Res C 99, 14–23. 10.1002/bdrc.21027.

Bao J, Tang C, Li J, Zhang Y, Bhetwal BP, Zheng H, et al. , 2014. RAN-Binding Protein 9 is Involved in Alternative Splicing and is Critical for Male Germ Cell Development and Male Fertility. Barsh GS, ed PLoS Genet. 10, e1004825; doi: 10.1371/journal.pgen.1004825. [PubMed: 25474150]

Bardullas U, Giordano M, Rodríguez VM, 2011. Chronic atrazine exposure causes disruption of the spontaneous locomotor activity and alters the striatal dopaminergic system of the male Sprague-Dawley rat. Neurotoxicol. Teratol. 33, 263–272. 10.1016/j.ntt.2010.09.001. [PubMed: 20850525]

Best JD, Berghmans S, Hunt JJFG, Clarke SC, Fleming A, Goldsmith P, Roach AG, 2008. Non-Associative Learning in Larval Zebrafish. Neuropsychopharmacol 33 (5), 1206–1215. 10.1038/sj.npp.1301489.

Bethsass J, Colangelo A, 2006. European Union Bans Atrazine, While the United States Negotiates Continued Use. Int. J. Occup. Environ. Health 12, 260–267. 10.1179/oeh.2006.12.3.260. [PubMed: 16967834]

Blanchard PE, Lerch RN, 2000. Watershed Vulnerability to Losses of Agricultural Chemicals: Interactions of Chemistry, Hydrology and Land Use. Environ. Sci. Technol. 34, 3315–3322.

Bridi D, Altenhofen S, Gonzalez JB, Reolon GK, Bonan CD, 2017. Glyphosate and Roundup® alter morphology and behavior in zebrafish. Toxicology 392, 32–39. 10.1016/j.tox.2017.10.007. [PubMed: 29032223]

Carnovali M, Banfi G, Mariotti M, 2019. Zebrafish Models of Human Skeletal Disorders: Embryo and Adult Swimming Together. Biomed Res. Int. 2019, 1–13. 10.1155/2019/1253710.

Chen K, Xiao H, Zeng J, Yu G, Zhou H, Huang C, et al. , 2017. Alternative Splicing of EZH2 pre-mRNA by SF3B3 Contributes to the Tumorigenic Potential of Renal Cancer. Clin. Cancer Res. 23, 3428–3441; doi:10.1158/1078-0432.CCR-16-2020. [PubMed: 27879367]

Chevrier C, Limon G, Monfort C, Rouget F, Garlantézec R, Petit C, Durand G, Cordier S, 2011. Urinary Biomarkers of Prenatal Atrazine Exposure and Adverse Birth Outcomes in the PELAGIE

Birth Cohort. Environ. Health Perspect. 119 (7), 1034–1041. 10.1289/ehp.1002775. [PubMed: 21367690]

Cleary JA, Tillitt DE, vom Saal FS, Nicks DK, Claunch RA, Bhandari RK, 2019. Atrazine induced transgenerational reproductive effects in medaka (Oryzias latipes). Environ. Pollut. 251, 639–650. 10.1016/j.envpol.2019.05.013. [PubMed: 31108297]

Cohen SP, LaChappelle AR, Walker BS, Lassiter CS, 2014. Modulation of estrogen causes disruption of craniofacial chondrogenesis in Danio rerio. Aquat. Toxicol. 152, 113–120. 10.1016/j.aquatox.2014.03.028. [PubMed: 24747083]

Cooper RL, 2000. Atrazine Disrupts the Hypothalamic Control of Pituitary-Ovarian Function. Toxicol. Sci. 53, 297–307. 10.1093/toxsci/53.2.297. [PubMed: 10696778]

Cox J, Mann M, 2008. MaxQuant enables high peptide identification rates, individualized ppb range mass accuracies and proteome-wide protein quantification. Nat. Biotechnol. 26, 1367–1372. 10.1038/nbt.1511. [PubMed: 19029910]

Cubbage CC, Mabee P, 1996. Development of the cranium and paired fins in the zebrafish Danio rerio (Ostariophysi, Cyprinidae). J. Morphol. 229, 121–160. [PubMed: 29852585]

Das BK, Xia L, Palandjian L, Gozani O, Chyung Y, Reed R, 1999. Characterization of a protein complex containing spliceosomal proteins SAPs 49, 130, 145, and 155. Mol Cell Biol 19, 6796–6802. 10.1128/MCB.19.10.6796. [PubMed: 10490618]

DeSesso JM, Scialli AR, White TEK, Breckenridge CB, 2014. Multigeneration Reproduction and Male Developmental Toxicity Studies on Atrazine in Rats: Reproductive Toxicity Studies of Atrazine. Birth Defects Res. B 101, 237–253. 10.1002/bdrb.21106.

dos Santos MJ, Vieira LG, Valdes SAC, Vilca FZ, Tornisielo VL, Santos ALQ, 2016. Effects of the exposure to atrazine on bone development of Podocnemis expansa (Testudines, Podocnemididae). Ecotoxicology 25, 594–600. 10.1007/s10646-016-1618-x. [PubMed: 26850621]

Ehrsam M, Knutie SA, Rohr JR, 2016. The herbicide atrazine induces hyperactivity and compromises tadpole detection of predator chemical cues: Atrazine reduces detection of predator chemical cues. Environ. Toxicol. Chem. 35, 2239–2244. 10.1002/etc.3377. [PubMed: 26799769]

Commission European, 2003. Review report for the active substance atrazine; European Commission Health and Consumer Protection Directorate-General. SANCO/10496/ 2003-final.

Fakan S, Leser G, Martin TE, 1984. Ultrastructural distribution of nuclear ribonucleoproteins as visualized by immunocytochemistry on thin sections. J. Cell Biol. 98, 358–363. 10.1083/jcb.98.1.358. [PubMed: 6231300]

Fitzgerald JA, Kirla KT, Zinner CP, vom Berg CM, 2019. Emergence of consistent intra-individual locomotor patterns during zebrafish development. Sci. Rep. 9: 13647. 10.1038/s41598-019-49614-y. [PubMed: 31541136]

Foradori CD, Healy JE, Zimmerman AD, Kemppainen RJ, Jones MA, Read CC, White BD, Yi KD, Hinds LR, Lacagnina AF, Quihuis AM, Breckenridge CB, Handa RJ, 2018. Characterization of Activation of the Hypothalamic-Pituitary-Adrenal Axis by the Herbicide Atrazine in the Female Rat. Endocrinology 159 (9), 3378–3388. 10.1210/en.2018-00474. [PubMed: 30060079]

Fraites MJP, Cooper RL, Buckalew A, Jayaraman S, Mills L, Laws SC, 2009. Characterization of the Hypothalamic-Pituitary-Adrenal Axis Response to Atrazine and Metabolites in the Female Rat. Toxicol. Sci. 112, 88–99. 10.1093/toxsci/kfp194. [PubMed: 19710361]

Freeman JL, Beccue N, Rayburn AL, 2005. Differential metamorphosis alters the endocrine response in anuran larvae exposed to T3 and atrazine. Aquat. Toxicol. 75, 263–276. 10.1016/j.aquatox.2005.08.012. [PubMed: 16213604]

Garcia GR, Noyes PD, Tanguay RL, 2016. Advancements in zebrafish applications for 21st century toxicology. Pharmacol. Ther. 161, 11–21. 10.1016/j.pharmthera.2016.03.009. [PubMed: 27016469]

Grande T, Young B, 2004. The ontogeny and homology of the Weberian apparatus in the zebrafish Danio rerio (Ostariophysi: Cypriniformes). Zool. J. Linn. Soc. 140, 241–254. 10.1111/j.1096-3642.2003.00097.x.

Guzzella L, Pozzoni F, Giuliano G, 2006. Herbicide contamination of surficial groundwater in Northern Italy. Environ. Pollut. 142, 344–353. 10.1016/j.envpol.2005.10.037. [PubMed: 16413952]

Hao C, Gely-Pernot A, Kervarrec C, Boudjema M, Becker E, Khil P, et al. , 2016. Exposure to the widely used herbicide atrazine results in deregulation of global tissue-specific RNA transcription in the third generation and is associated with a global decrease of histone trimethylation in mice. Nucleic Acids Res. gkw840; doi: 10.1093/nar/gkw840.

Heindel JJ, Vandenberg LN, 2015. Developmental origins of health and disease: a paradigm for understanding disease cause and prevention. Curr. Opin. Pediatr. 27, 248–253. 10.1097/MOP.0000000000000191. [PubMed: 25635586]

Horzmann KA, Freeman JL, 2018. Making Waves: New Developments in Toxicology With the Zebrafish. Toxicol. Sci. 163, 5–12. 10.1093/toxsci/kfy044. [PubMed: 29471431]

Horzmann KA, Reidenbach LS, Thanki DH, Winchester AE, Qualizza BA, Ryan GA, Egan KE, Hedrick VE, Sobreira TJP, Peterson SM, Weber GJ, Wirbisky-Hershberger SE, Sepúlveda MS, Freeman JL, 2018. Embryonic atrazine exposure elicits proteomic, behavioral, and brain abnormalities with developmental time specific gene expression signatures. J. Proteomics 186, 71–82. 10.1016/j.jprot.2018.07.006. [PubMed: 30012420]

Horzmann KA, Lin LF, Taslakjian B, Yuan C, Freeman JL, 2021. Embryonic atrazine exposure and later in life behavioral and brain transcriptomic, epigenetic, and pathological alterations in adult male zebrafish. Cell Biol. Toxicol. 37, 421–439. 10.1007/s10565-020-09548-y. [PubMed: 32737625]

Horzmann KA, Lin LF, Taslakjian B, Yuan C, Freeman JL, 2022. Anxiety-related behavior and associated brain transcriptome and epigenome alterations in adult female zebrafish exposed to atrazine during embryogenesis. Chemosphere 308, 136431. 10.1016/j.chemosphere.2022.136431. [PubMed: 36126741]

Huang P, Yang J, Song Q, 2014. Atrazine Affects Phosphoprotein and Protein Expression in MCF-10A Human Breast Epithelial Cells. IJMS 15, 17806–17826. 10.3390/ijms151017806. [PubMed: 25275270]

Inoue M, Tanimoto M, Oda Y, 2013. The role of ear stone size in hair cell acoustic sensory transduction. Sci. Rep. 3, 2114. 10.1038/srep02114. [PubMed: 23817603]

Jackson GC, Mittaz-Crettol L, Taylor JA, Mortier GR, Spranger J, Zabel B, Le Merrer M, Cormier-Daire V, Hall CM, Offiah A, Wright MJ, Savarirayan R, Nishimura G, Ramsden SC, Elles R, Bonafe L, Superti-Furga A, Unger S, Zankl A, Briggs MD, 2012. Pseudoachondroplasia and multiple epiphyseal dysplasia: A 7-year comprehensive analysis of the known disease genes identify novel and recurrent mutations and provides an accurate assessment of their relative contribution. Hum. Mutat. 33 (1), 144–157. 10.1002/humu.21611. [PubMed: 21922596]

Joshi N, Rhoades MG, Bennett GD, Wells SM, Mirvish SS, Breitbach MJ, Shea PJ, 2013. Developmental Abnormalities in Chicken Embryos Exposed to N-Nitrosoatrazine. J. Toxic. Environ. Health A 76 (17), 1015–1022. 10.1080/15287394.2013.831721.

Kimmel CB, Miller CT, Kruze G, Ullmann B, BreMiller RA, Larison KD, Snyder HC, 1998. The Shaping of Pharyngeal Cartilages during Early Development of the Zebrafish. Dev. Biol. 203 (2), 245–263. 10.1006/dbio.1998.9016. [PubMed: 9808777]

Kuratani S, Matsuo I, Aizawa S. Developmental patterning and evolution of the mammalian viscerocranium: Genetic insights into comparative morphology. 17.

Kwon RY, Watson CJ, Karasik D, 2019. Using zebrafish to study skeletal genomics. Bone 126, 37–50. 10.1016/j.bone.2019.02.009. [PubMed: 30763636]

LeBaron HM, McFarland JE, Burnside OC, 2008. The Triazine Herbicides. Elsevier.

Legrand JMD, Chan A-L, La HM, Rossello FJ, Änkö M-L, Fuller-Pace FV, ¨ et al. , 2019. DDX5 plays essential transcriptional and post-transcriptional roles in the maintenance and function of spermatogonia. Nat. Commun. 10, 2278. 10.1038/s41467-019-09972-7. [PubMed: 31123254]

Lenkowski JR, McLaughlin KA, 2010. Acute atrazine exposure disrupts matrix metalloproteinases and retinoid signaling during organ morphogenesis in Xenopus laevis. J. Appl. Toxicol. 30, 582–589. 10.1002/jat.1529. [PubMed: 20809547]

Li B, Jiang Y, Xu Y, Li Y, Li B, 2019. Identification of miRNA-7 as a regulator of brain-derived neurotrophic factor/α-synuclein axis in atrazine-induced Parkinson's disease by peripheral blood and brain microRNA profiling. Chemosphere 233, 542–548. 10.1016/j.chemosphere.2019.05.064. [PubMed: 31185338]

Lim S, Ahn SY, Song IC, Chung MH, Jang HC, Park KS, Lee K-U, Pak YK, Lee HK, Malaga G, 2009. Chronic Exposure to the Herbicide, Atrazine, Causes Mitochondrial Dysfunction and Insulin Resistance. PLoS One 4 (4), e5186. 10.1371/journal.pone.0005186. [PubMed: 19365547]

Lin Z, Dodd CA, Xiao S, Krishna S, Ye X, Filipov NM, 2014. Gestational and Lactational Exposure to Atrazine via the Drinking Water Causes Specific Behavioral Deficits and Selectively Alters Monoaminergic Systems in C57BL/6 Mouse Dams, Juvenile and Adult Offspring. Toxicol. Sci. 141, 90–102. 10.1093/toxsci/kfu107. [PubMed: 24913803]

Luo S, Yang Y, Chen J, Zhong Z, Huang H, Zhang J, Cui L, 2016. Tanshinol stimulates bone formation and attenuates dexamethasone-induced inhibition of osteogenesis in larval zebrafish. J. Orthopaedic Translation 4, 35–45. 10.1016/j.jot.2015.07.002.

Ma K, Wu H-Y, Zhang B, He X, Li B-X, 2015. Neurotoxicity effects of atrazine-induced SH-SY5Y human dopaminergic neuroblastoma cells via microglial activation. Mol. Biosyst. 11, 2915–2924. 10.1039/C5MB00432B. [PubMed: 26256823]

McBirney M, King SE, Pappalardo M, Houser E, Unkefer M, Nilsson E, Sadler-Riggleman I, Beck D, Winchester P, Skinner MK, Óvilo C, 2017. Atrazine induced epigenetic transgenerational inheritance of disease, lean phenotype and sperm epimutation pathology biomarkers. PLoS One 12 (9), e0184306. 10.1371/journal.pone.0184306. [PubMed: 28931070]

Meffe R, de Bustamante I, 2014. Emerging organic contaminants in surface water and groundwater: A first overview of the situation in Italy. Sci. Total Environ. 481, 280–295. 10.1016/j.scitotenv.2014.02.053. [PubMed: 24602913]

Metselaar PI, Hos C, Welting O, Bosch JA, Kraneveld AD, de Jonge WJ, Te Velde AA, 2021. Ambiguity about Splicing Factor 3b Subunit 3 (SF3B3) and Sin3A Associated Protein 130 (SAP130). Cells 10 (3), 590. 10.3390/cells10030590. [PubMed: 33800128]

Migeot V, Albouy-Llaty M, Carles C, Limousi F, Strezlec S, Dupuis A, Rabouan S, 2013. Drinking-water exposure to a mixture of nitrate and low-dose atrazine metabolites and small-for-gestational age (SGA) babies: A historic cohort study. Environ. Res. 122, 58–64. 10.1016/j.envres.2012.12.007. [PubMed: 23340115]

Mork L, Crump G, 2015. Zebrafish Craniofacial Development. In: Current Topics in Developmental Biology, Vol. 115. Elsevier, pp. 235–269. [PubMed: 26589928]

Pantoja C, Hoagland A, Carroll EC, Karalis V, Conner A, Isacoff EY, 2016. Neuromodulatory Regulation of Behavioral Individuality in Zebrafish. Neuron 91, 587–601. 10.1016/j.neuron.2016.06.016. [PubMed: 27397519]

Paul S, Schindler S, Giovannone D, Terrazzani A de M, Mariani FV, Crump JG, 2016. Ihha induces hybrid cartilage-bone cells during zebrafish jawbone regeneration. 11.

Peterson SM, Zhang J, Weber G, Freeman JL, 2011. Global Gene Expression Analysis Reveals Dynamic and Developmental Stage-Dependent Enrichment of Lead-Induced Neurological Gene Alterations. Environ. Health Perspect. 119, 615–621. 10.1289/ehp.1002590. [PubMed: 21147602]

Peterson SM, Zhang J, Freeman JL, 2013. Developmental reelin expression and time point-specific alterations from lead exposure in zebrafish. Neurotoxicol. Teratol. 38, 53–60. 10.1016/j.ntt.2013.04.007. [PubMed: 23665418]

Pettersson M, Vaz R, Hammarsjö A, Eisfeldt J, Carvalho CMB, Hofmeister W, Tham E, Horemuzova E, Voss U, Nishimura G, Klintberg B.o., Nordgren A, Nilsson D, Grigelioniene G, Lindstrand A, 2018. *Alu-Alu* mediated intragenic duplications in *IFT81* and *MATN3* are associated with skeletal dysplasias. Hum. Mutat. 39 (10), 1456–1467. 10.1002/humu.23605. [PubMed: 30080953]

Pullig O, Weseloh G, Klatt AR, Wagener R, Swoboda B, 2002. Matrilin-3 in human articular cartilage: increased expression in osteoarthritis. Osteoarthr. Cartil. 10, 253–263. 10.1053/joca.2001.0508.

Riley BB, Moorman SJ, 2000. Development of utricular otoliths, but not saccular otoliths, is necessary for vestibular function and survival in zebrafish. J. Neurobiol. 43, 329–337. [PubMed: 10861559]

Russart KLG, Rhen T, 2016. Atrazine alters expression of reproductive and stress genes in the developing hypothalamus of the snapping turtle, Chelydra serpentina. Toxicology 366–367, 1–9. 10.1016/j.tox.2016.08.001.

Staal YCM, Meijer J, van der Kris RJC, de Bruijn AC, Boersma AY, Gremmer ER, Zwart EP, Beekhof PK, Slob W, van der Ven LTM, 2018. Head skeleton malformations in zebrafish (Danio rerio)

to assess adverse effects of mixtures of compounds. Arch. Toxicol. 92 (12), 3549–3564. 10.1007/s00204-018-2320-y. [PubMed: 30288550]

Stayner LT, Almberg K, Jones R, Graber J, Pedersen M, Turyk M, 2017. Atrazine and nitrate in drinking water and the risk of preterm delivery and low birth weight in four Midwestern states. Environ. Res. 152, 294–303. 10.1016/j.envres.2016.10.022. [PubMed: 27816866]

Stradtman SC, Freeman JL, 2021. Mechanisms of neurotoxicity associated with exposure to the herbicide atrazine. Toxics 9, 207. 10.3390/toxics9090207. [PubMed: 34564358]

TeSlaa JJ, Keller AN, Nyholm MK, Grinblat Y, 2013. Zebrafish Zic2a and Zic2b regulate neural crest and craniofacial development. Dev. Biol. 380, 73–86. 10.1016/j.ydbio.2013.04.033. [PubMed: 23665173]

Ton C, Lin Y, Willett C, 2006. Zebrafish as a model for developmental neurotoxicity testing. Birth Defect Res. A 76, 553–567. 10.1002/bdra.20281.

Walker M, Kimmel C, 2007. A two-color acid-free cartilage and bone stain for zebrafish larvae. Biotech. Histochem. 82, 23–28. 10.1080/10520290701333558. [PubMed: 17510811]

Walker BS, Kramer AG, Lassiter CS, 2018. Atrazine affects craniofacial chondrogenesis and axial skeleton mineralization in zebrafish (Danio rerio). Toxicol. Ind. Health 34, 329–338. 10.1177/0748233718760419. [PubMed: 29575980]

Waller SA, Paul K, Peterson SE, Hitti JE, 2010. Agricultural-related chemical exposures, season of conception, and risk of gastroschisis in Washington State. Am. J. Obstet. Gynecol. 202, 241.e1–241.e6. 10.1016/j.ajog.2010.01.023.

Wang D, Li B, Wu Y, Li B, 2019. The Effects of Maternal Atrazine Exposure and Swimming Training on Spatial Learning Memory and Hippocampal Morphology in Offspring Male Rats via PSD95/NR2B Signaling Pathway. Cell. Mol. Neurobiol. 39, 1003–1015. 10.1007/s10571-019-00695-3. [PubMed: 31187311]

Weber GJ, Sepúlveda MS, Peterson SM, Lewis SS, Freeman JL, 2013. Transcriptome Alterations Following Developmental Atrazine Exposure in Zebrafish Are Associated with Disruption of Neuroendocrine and Reproductive System Function, Cell Cycle, and Carcinogenesis. Toxicol. Sci. 132, 458–466. 10.1093/toxsci/kft017. [PubMed: 23358194]

Winchester PD, Huskins J, Ying J, 2009. Agrichemicals in surface water and birth defects in the United States. Acta Paediatr. 98, 664–669. 10.1111/j.1651-2227.2008.01207.x. [PubMed: 19183116]

Wirbisky SE, Weber GJ, Sepúlveda MS, Xiao C, Cannon JR, Freeman JL, 2015. Developmental origins of neurotransmitter and transcriptome alterations in adult female zebrafish exposed to atrazine during embryogenesis. Toxicology 333, 156–167. 10.1016/j.tox.2015.04.016. [PubMed: 25929836]

Wirbisky SE, Weber GJ, Schlotman KE, Sepúlveda MS, Freeman JL, 2016a. Embryonic atrazine exposure alters zebrafish and human miRNAs associated with angiogenesis, cancer, and neurodevelopment. Food Chem. Toxicol. 98, 25–33. 10.1016/j.fct.2016.03.027. [PubMed: 27046698]

Wirbisky SE, Weber GJ, Sepúlveda MS, Lin T-L, Jannasch AS, Freeman JL, 2016b. An embryonic atrazine exposure results in reproductive dysfunction in adult zebrafish and morphological alterations in their offspring. Sci. Rep. 6 10.1038/srep21337.

World Health Orgnanization, 2011. Atrazine and its metabolites in drinking-water. WHO Press, Geneva, Switzerland. https://cdn.who.int/media/docs/default-source/wash-documents/wash-chemicals/antrazine.pdf?sfvrsn=aed2ccc7_4.

Yao Q, DeSmidt AA, Tekin M, Liu X, Lu Z, 2016. Hearing Assessment in Zebrafish During the First Week Postfertilization. Zebrafish 13, 79–86. 10.1089/zeb.2015.1166. [PubMed: 26982161]

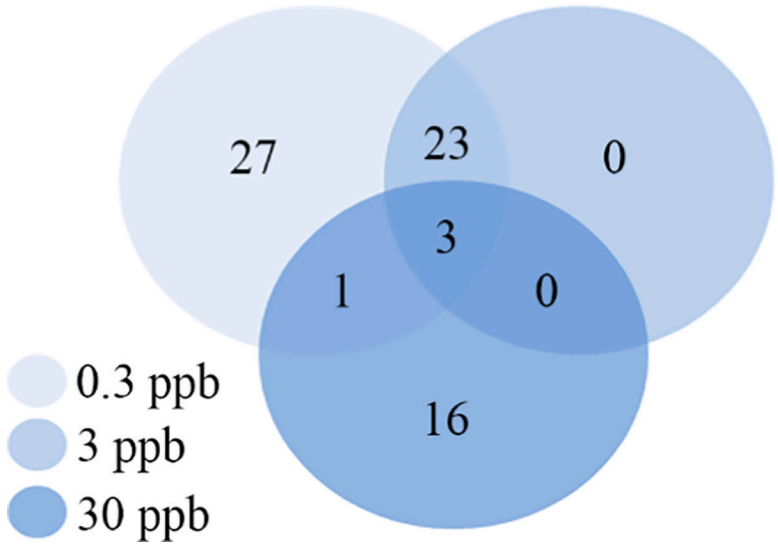

Fig. 1. A Venn diagram of proteins altered within treatment groups.

ATZ F1 larvae in the 0.3 ppb treatment group had 54 proteins altered, in the 3 ppb treatment group had 26 proteins altered, and in the 30 ppb treatment group had 20 proteins altered. 24 proteins were altered in two treatment groups (23 proteins in the 0.3 and 3 ppb and 1 protein in the 0.3 and 30 ppb treatment groups) and 3 proteins were altered in all three treatment groups (HBE1, MATN3, and SF3B3).

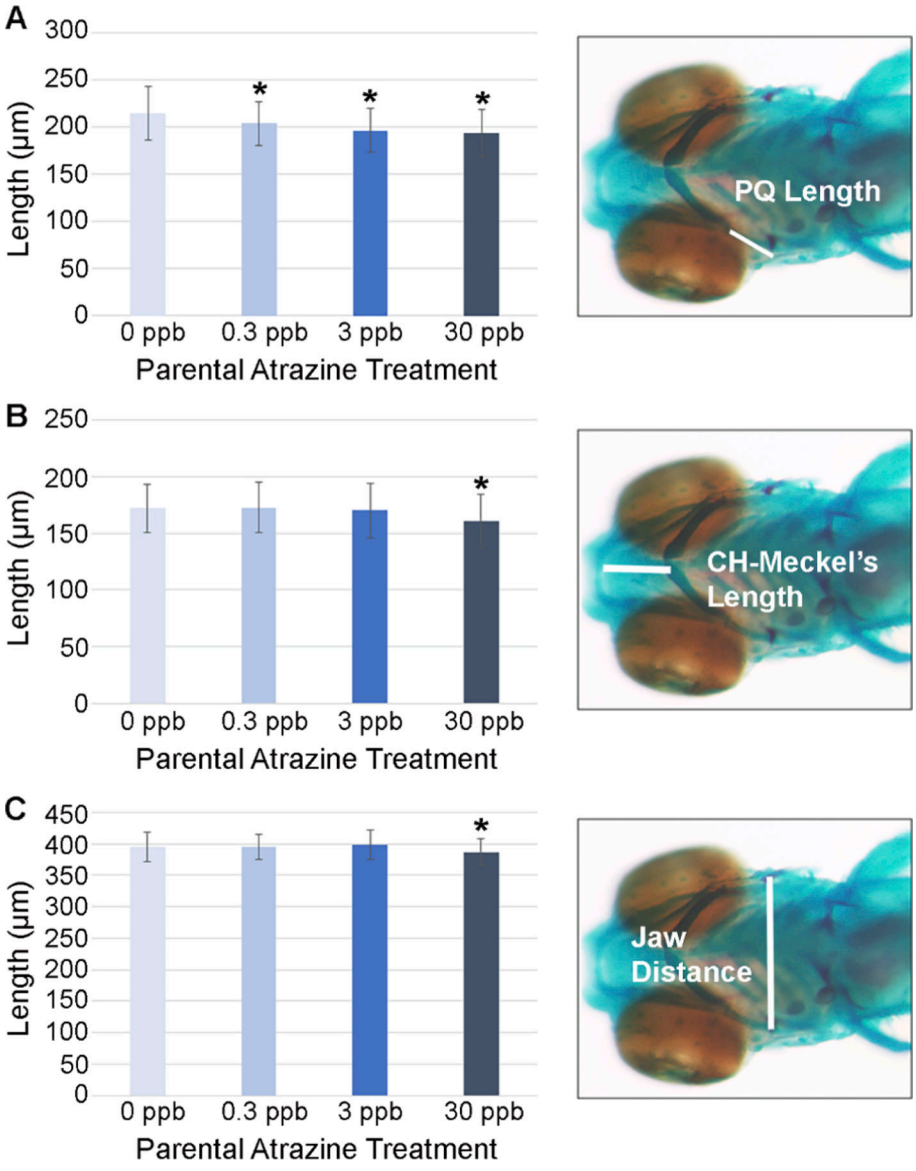

Fig. 2. Significant alterations in cartilage measurements in ATZ F1 larvae at 120 hpf.

ATZ F1 larvae of all treatment groups had significantly shorter PQ length (A). CH-Meckel's length was shorter for 30 ppb F1 groups (B). Jaw distance was also shorter for 30 ppb F1 larvae (C). White lines indicate how each parameter was measured in right panels. For each ATZ F1 treatment group 11–20 larvae were imaged as subsamples per biological replicate. A total of 5 biological replicates were assessed to achieve 55–75 larvae per treatment group. *$p < 0.05$. Error bars represent standard deviation.

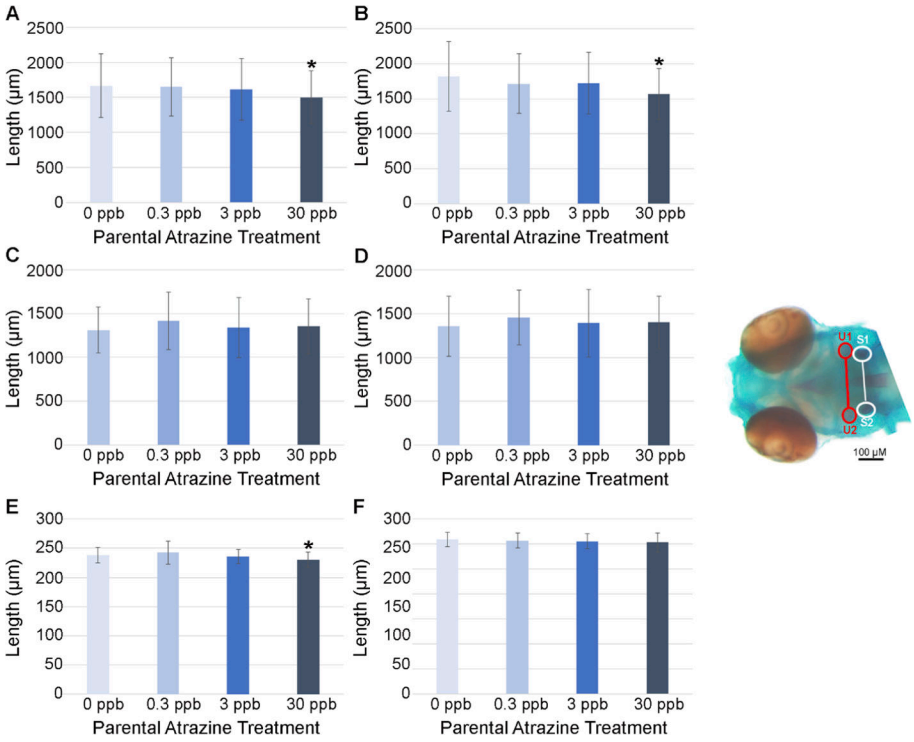

Fig. 3. Otolith positioning and surface area measurements in ATZ F1 larvae at 120 hpf.

Otoliths are labeled as utricular (U) 1 or 2 for the anterior otoliths (red) and saccular (S) 1 or 2 for the posterior otoliths (white). Saccular otolith Area 1 (A) and saccular otolith area 2 (B) were significantly smaller in F1 30 ppb progeny. No change in surface area was found for utricular otolith area 1 (C) or utricular otolith area 2 (D). Length between saccular otoliths was significantly shorter in F1 30 ppb fish (E), but no significant difference in length was observed between utricular otoliths (F). For each ATZ F1 treatment group 11–20 larvae were imaged as subsamples per biological replicate. A total of 5 biological replicates were assessed to achieve 55–75 larvae per treatment group. *$p < 0.05$. Error bars represent standard deviation. Scale bar is 100 µM.

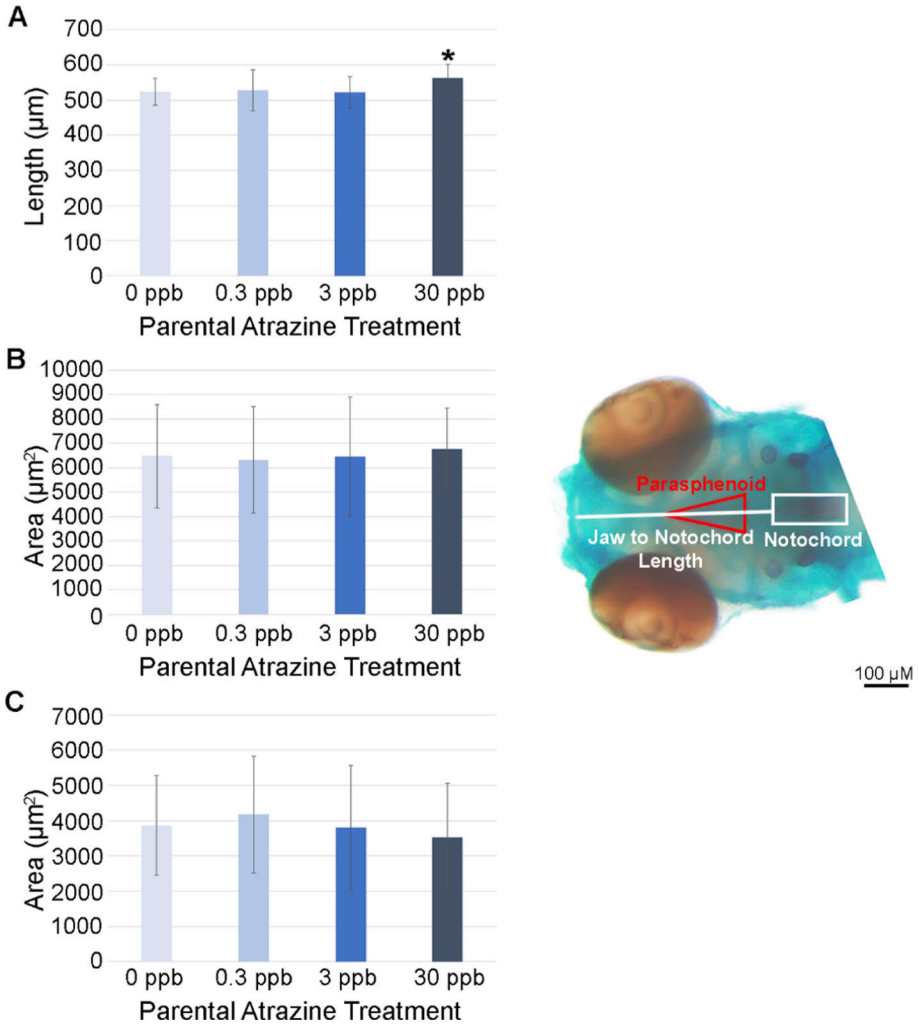

Fig. 4. Jaw to notochord length and notochord and parasphenoid surface area in ATZ F1 larvae at 120 hpf.

Jaw to notochord length was significantly increased in F1 30 ppb larvae (A) (white line). There were no differences among the offspring of the different parental atrazine treatment groups for the notochord (B) (white rectangle) or parasphenoid (C) (red triangle) surface area. For each ATZ F1 treatment group 11–20 larvae were imaged as subsamples per biological replicate. A total of 5 biological replicates were assessed to achieve 55–75 larvae per treatment group. *$p < 0.05$. Error bars represent standard deviation. Scale bar is 100 μM.

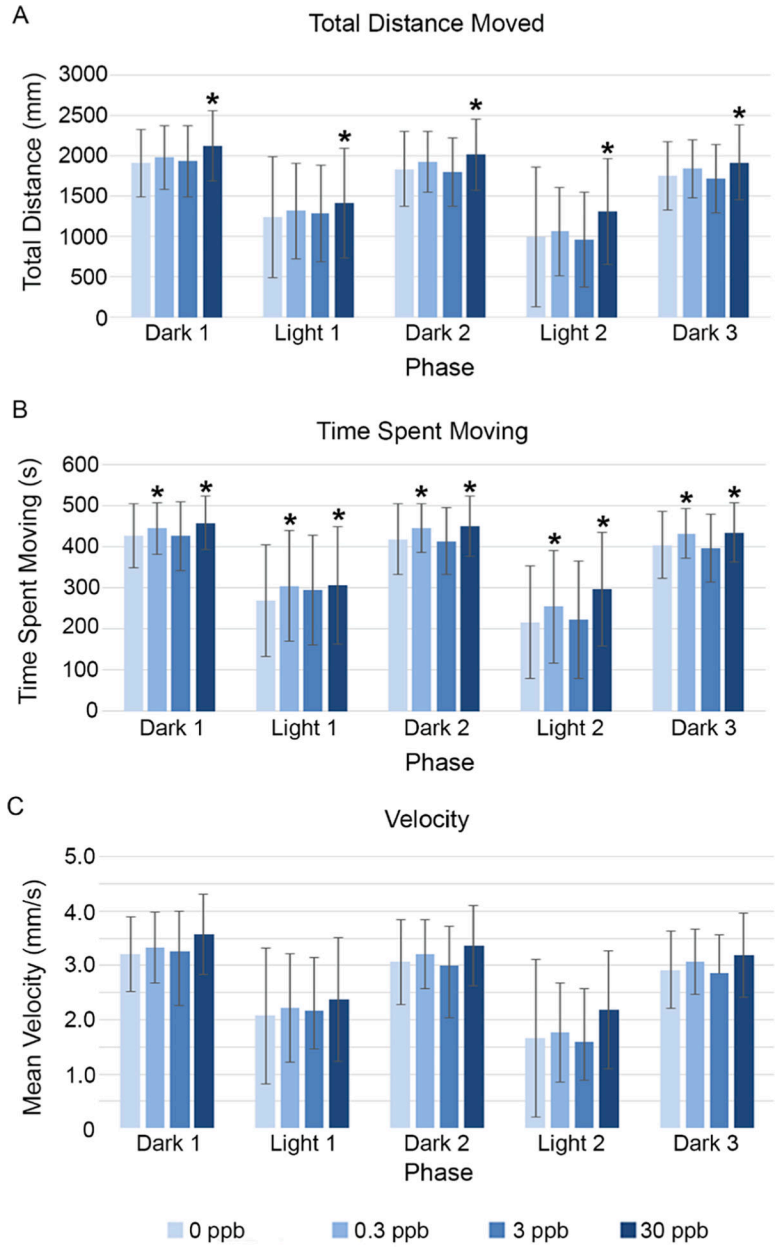

Fig. 5. Phasic behavior in ATZ F1 larvae at 120 hpf.

An increase in total distance moved in the 30 ppb F1 fish was seen in all light and dark phases (A). An increase in time spent moving was observed in the 0.3 and 30 ppb F1 larvae in all phases (B). No significant differences were detected for velocity (C). Each treatment group had 8 biological replicates containing 24 subsample fish per biological replicate for a total of 192 fish per treatment group. *$p < 0.05$. Error bars represent standard deviation.

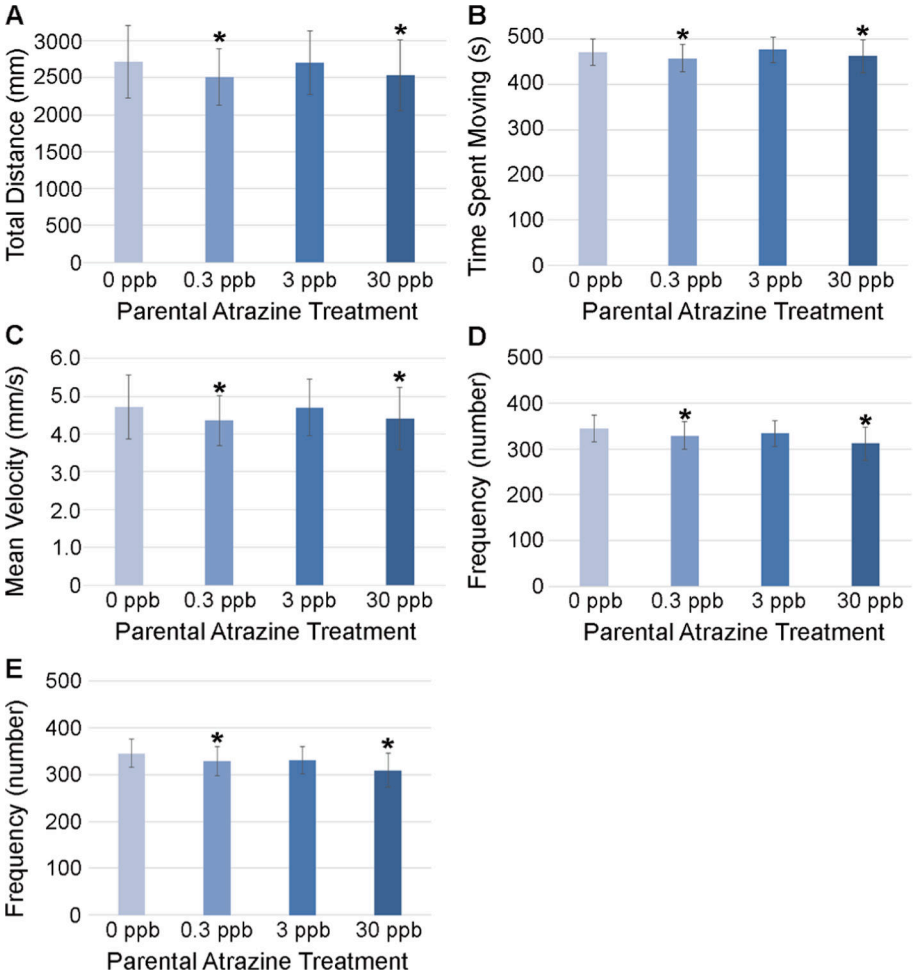

Fig. 6. Acoustic startle behavior in ATZ F1 larvae at 144 hpf.

A decrease in total distance moved (A), time spent moving (B), velocity (C), counterclockwise turns (D), and clockwise turns (E) in the 0.3 and 30 ppb F1 fish was observed. Each treatment group had 5 biological replicates containing 24 subsample fish per biological replicate for a total of 120 fish per treatment group. *$p < 0.05$. Error bars represent standard deviation.

Table 1

A list of the 70 uniquely mapped proteins altered with parental ATZ exposure.

Symbol	Entrez Gene Name	Ensembl/GenPept/UniProt/ Swiss-Prot Accession	0.3 ppb/ 0 ppb Fold Change	3 ppb/ 0 ppb Fold Change	30 ppb/ 0 ppb Fold Change
2310057J18Rik	RIKEN cDNA 2310057J18 gene	A5PF61			0.577
Actn3	actinin alpha 3	Q6P0J5			0.793
ACTR2	actin related protein 2	F1QF15	0.344		
ADD3	adducin 3	F1R6L1	0.411		
ADSS1	adenylosuccinate synthase 1	ENSG00000185100			0.462
AGRN	agrin	F1R074	−0.837	−1.244	
ANXA11	annexin A11	Q804G3	0.366		
ATP1B2	ATPase Na+/K + transporting subunit beta 2	Q9DGL2	−0.26	−0.474	
ATP5F1A	ATP synthase F1 subunit alpha	Q58P23	0.981		
ATP5F1C	ATP synthase F1 subunit gamma	Q6P959	1.192	1.34	
ATP5MD	ATP synthase membrane subunit DAPIT	ENSG00000173915	−1.109		
ATP5ME	ATP synthase membrane subunit e	ENSG00000169020	−7.41	−7.41	
ATP5MG	ATP synthase membrane subunit g	Q6P6E0	0.465		
ATP5PB	ATP synthase peripheral stalk-membrane subunit b	Q5XJJ3	0.563	0.682	
ATP6V1E1	ATPase H + transporting V1 subunit E1	Q6NWK4	0.706	1.081	
CAPNS1	calpain small subunit 1	X1WFZ2			0.883
CES1	carboxylesterase 1	Q1LYL6			0.614
COL10A1	collagen type X alpha 1 chain	F1QXD5	−6.009	−0.658	
COL18A1	collagen type XVIII alpha 1 chain	ENSG00000182871	−0.448	−0.531	
COL1A1	collagen type I alpha 1 chain	ENSG00000108821			−0.852
CRYBA2	crystallin beta A2	Q6IQU2	−0.52	−0.541	
CRYBB1	crystallin beta B1	Q90WT1	−0.721		
EPRS1	glutamyl-prolyl-tRNA synthetase 1	A8WG07	0.418	0.511	
FAU	FAU ubiquitin like and ribosomal protein S30 fusion	Q6PC01	0.483		
GAPDHS	glyceraldehyde-3-phosphate dehydrogenase, spermatogenic	F1R3D3	0.62	0.515	
GATM	glycine amidinotransferase	ENSG00000171766	0.498		
GNB1	G protein subunit beta 1	Q803H5	0.312		

Symbol	Entrez Gene Name	Ensembl/GenPept/UniProt/ Swiss-Prot Accession	0.3 ppb/ 0 ppb Fold Change	3 ppb/ 0 ppb Fold Change	30 ppb/ 0 ppb Fold Change
HBE1	hemoglobin subunit epsilon 1	Q5BLF6	0.485	0.573	0.344
HMGB1	high mobility group box 1	ENSG00000189403	−0.436		
HNRNPM	heterogeneous nuclear ribonucleoprotein M	ENSG00000099783			5.332
HNRNPR	heterogeneous nuclear ribonucleoprotein R	ENSG00000125944			0.339
HNRNPU	heterogeneous nuclear ribonucleoprotein U	Q6PYX3	−6.771		
HSPD1	heat shock protein family D (Hsp60) member 1	Q803B0	1.28	0.946	
IGFN1	immunoglobulin like and fibronectin type III domain containing 1	ENSG00000163395			0.282
ILF2	interleukin enhancer binding factor 2	Q6NZ06			0.956
KRT17	keratin 17	Q6DHU3	−0.387		
LUM	lumican	Q6IQQ7			−0.298
MARCKSL1	MARCKS like 1	ENSG00000175130	−1.522	−1.575	
MATN3	matrilin 3	ENSG00000132031	0.569	0.985	0.706
MDH1	malate dehydrogenase 1	Q7ZSY2	−0.725	−1.316	
MYL12A	myosin light chain 12A	Q6PHJ8	−7.32	−0.693	
NID1	nidogen 1	F1RAG3			−0.585
NOMO1 (includes others)	NODAL modulator 1	ENSG00000103512			−0.252
OPN1LW	opsin 1, long wave sensitive	A0A0N9P0E6	−1.298		
OPN1SW	opsin 1, short wave sensitive	Q6P981	−0.732		
PC	pyruvate carboxylase	Q7ZZ22			0.8
PFN1	profilin 1	ENSG00000108518	−0.409		
PHB2	prohibitin 2	Q6PC13	0.504		
PRPF8	pre-mRNA processing factor 8	A0A0R4J8E6	0.329	0.387	
PRSS2	serine protease 2	Q7SX90	0.767		
RAB10	RAB10, member RAS oncogene family	Q6DGV5	0.329		0.304
REELD1	reeler domain containing 1	ENSG00000250673	−0.907	−1.133	
RHO	rhodopsin	ENSG00000163914	−1.09		
RPL10A	ribosomal protein L10a	Q6PC69			−0.585
RPL11	ribosomal protein L11	Q6IQI6	0.483		
RPL17-C18orf32	RPL17-C18orf32	Q7T1K0	0.559	0.478	
RPL3	ribosomal protein L3	Q5BJJ2	1.001		

Symbol	Entrez Gene Name	Ensembl/GenPept/UniProt/ Swiss-Prot Accession	0.3 ppb/ 0 ppb Fold Change	3 ppb/ 0 ppb Fold Change	30 ppb/ 0 ppb Fold Change
RPL4	ribosomal protein L4	Q1LUY6	0.721		
RPS11	ribosomal protein S11	Q7ZV05	0.543		
RPS16	ribosomal protein S16	Q1LWH1	1.337	1.195	
Rps3a1	ribosomal protein S3A1	Q6PBY1	0.883	0.773	
S100A10	S100 calcium binding protein A10	Q7ZVA4	−0.617		
S100A4	S100 calcium binding protein A4	Q6XG62	1.83	2.669	
SF3B3	splicing factor 3b subunit 3	Q1LVE8	−0.498	−0.475	−0.439
SLC25A12	solute carrier family 25 member 12	A0A0R4II73	0.421	0.412	
SNRPG	small nuclear ribonucleoprotein polypeptide G	Q66I63	0.628		
SSR3	signal sequence receptor subunit 3	B8JL82	0.263		
TMEM38A	transmembrane protein 38A	Q6P2T0	−0.635	−0.785	
TNNI2	troponin I2, fast skeletal type	Q71N42	−1.227		
VSNL1	visinin like 1	E7FCW3			0.498

Table 2

Top physiological system development and function pathways altered in progeny at 120 hpf.

Physiological System Development and Function Pathway	p-value[a]	Number of molecules[b]
Progeny of 0.3 ppb treatment group		
Embryonic development	4.73E–02–4.44E–04	7
Nervous system development and function	4.73E–02–4.44E–04	6
Organ development	4.96E–02–4.44E–04	7
Organ morphology	4.96E–02–4.44E–04	6
Organismal development	4.73E–02–4.44E–04	7
Progeny of 3 ppb treatment group		
Embryonic development	4.64E–02–1.53E–04	7
Nervous system development and function	4.95E–02–1.53E–04	8
Organ development	4.95E–02–1.53E–04	7
Organ morphology	4.95E–02–1.53E–04	9
Organismal development	4.95E–02–1.53E–04	8

[a] Derived from the likelihood of observing the degree of enrichment in a protein set of a given size by chance alone.

[b] Classified as being differentially expressed that relate to the specified function category; a protein may be present in more than one category.

Table 3

Top diseases and disorders pathways altered in progeny at 120 hpf.

Diseases and Disorders Pathway	p-value[a]	Number of molecules[b]
Progeny of 0.3 ppb treatment group		
Neurological disease	3.83E–02–1.98E–06	11
Organismal injury and abnormalities	4.90E–02–1.98E–06	14
Psychological disorders	3.74E–02–1.98E–06	9
Hereditary disorder	4.90E–02–3.80E–06	9
Skeletal and muscular disorders	4.67E–02–3.80E–06	12
Progeny of 3 ppb treatment group		
Neurological disease	5.00E–02–3.57E–06	18
Organismal injury and abnormalities	5.00E–02–3.57E–06	25
Cancer	4.55E–02–1.31E–05	24
Tumor morphology	2.16E–03–1.31E–05	5
Ophthalmic disease	4.95E–02–1.53E–04	7

[a] Derived from the likelihood of observing the degree of enrichment in a protein set of a given size by chance alone.

[b] Classified as being differentially expressed that relate to the specified function category; a protein may be present in more than one category.

Table 4

Morphology measurements in larval offspring at 120 hpf.

Parental ATZ treatment group	Body length (μm) ± SD[a]	Head length (μm) ± SD	Head width (μm) ± SD	Brain length (μm) ± SD	Head length/body length ratio ± SD	Head width/ body length ratio ± SD	Brain length/ total length ratio ± SD
0 ppb	4270 ± 218	767 ± 61	692 ± 59	947 ± 59	0.181 ± 0.013	0.163 ± 0.016	0.222 ± 0.013
0.3 ppb	4311 ± 170	792 ± 45*	683 ± 34	949 ± 52	0.184 ± 0.009*	0.159 ± 0.008	0.221 ± 0.015
3 ppb	4266 ± 208	780 ± 65	692 ± 51	954 ± 52	0.183 ± 0.013	0.162 ± 0.012	0.224 ± 0.015
30 ppb	4274 ± 185	795 ± 50*	680 ± 47	946 ± 46	0.186 ± 0.008*	0.159 ± 0.011	0.222 ± 0.012

*$p < 0.05$ compared to progeny of the 0 ppb treatment group (no parental ATZ exposure).

[a]Standard deviation.

Table 5

C bend reaction time by tap at 144 hpf.

Parental ATZ treatment group	Tap 1	Tap 2	Tap 3	Tap 4
0 ppb	0.237	0.171	0.340	0.287
0.3 ppb	0.300	0.216	0.445	0.286
3 ppb	0.258	0.175	0.300	0.275
30 ppb	0.189	0.208	0.353	0.171 *

* $p < 0.05$ compared to progeny of the 0 ppb treatment group (no parental ATZ exposure).